Optimal Strategy to Model the Electrodialytic Recovery of Some Fermentation Products

Mark Spitz (mspitz@unibus.it)
Dept. Food Science and Technology, University of XXX, VYUUU, Italy
Tutor: Prof. X Y

This PhD thesis dealt with the assessment of a comprehensive mathematical model of the electrodialytic (ED) recovery of some sodium salts of mono-carboxylic acids from aqueous solutions and establishment of an experimental procedure to determine the effective parameters for designing and optimising ED stacks.

Strategia ottimale per la modellizzazione del recupero elettrodialitico di alcuni prodotti di fermentazione

Questa tesi di dottorato ha riguardato lo sviluppo di un modello matematico per il recupero elettrodialitico (ED) di alcuni sali sodici di acidi monocarbossilici da soluzioni acquose e di una procedura sperimentale diretta alla determinazione dei parametri essenziali per la progettazione e l'ottimizzazione di unità di ED.

Key words: Electrodialysis; organic acids; modelling; transport numbers in solution and electro-membranes.

1. Introduction

In accordance with the PhD thesis project previously decribed (Spitz, 2004), this oral communication reports the main results of the following four activities directed to:

A1) determine and model the density (ρ), kinematic viscosity (ν), and electric conductivity (χ) of sodium chloride, acetate (A), and lactate (L) in aqueous solutions as functions of solute concentration (C_B);
A2) assess and model the ED processes in a pilot-plant scale equipped with monopolar membranes as functions of current density (I), feed flow rate (Q_F) and C_B;
A3) establish an experimental procedure to determine the effective design parameters for ED stacks;
A4) assess the really important parameters in ED stack design and optimisation.

2. Electrodialysis Applications

Electrodialysis (ED) is a unit operation for the separation or concentration of ions in solutions based upon their selective electro-migration through semipermeable membranes under the influence of a potential gradient (Ho and Sirkar, 1992). ED was commercially introduced to desalinate water about 10 years before reverse osmosis (RO). The production of potable water from brackish water is currently the most important industrial ED application. Also the production of table salt from seawater has achieved a certain commercial importance, especially in Japan and Kuwait, even if it seems to be highly subsidized (Ho and Sirkar, 1992). Despite the first industrial ED application in the food sector dated back to 1960 and concerned the demineralisation of cheese whey for use in baby-foods, other applications concerning tartaric wine stabilization of wine, fruit juice de-acidification, and molasses desalting are gaining increasing importance with large-scale industrial plants.

Table 1 *Main applications of the ED in the food sector*.

Application	Example
Fractionation	Brackish water desalination
	Nitrate removal from drinking water
	NaCl removal from amino acid solutions
	Cheese whey demineralisation
	Desalting of protein hydrolysates (i.e., soy sauce), sugar solutions, molasses, and polysaccharide dispersions
	De-acidification of fruit juices
	Tartaric wine stabilisation
	Flavour recover from pickle brines
Concentration	Edible table salt production from seawater
	Salts of organic acids from exhausted fermentation media
	Amino acids from protein hydrolysates
Splitting	Conversion of salts into the corresponding free acid and base

The fermentation industry is also interested, especially when the main product of the microbial metabolism is an electrolyte which can inhibit the cell growth and/or metabolite production in either its free or dissociated form, or is dissolved in media rich of impurities removable via numerous and expensive purification steps. In these cases, ED was for instance suggested as an environmentally-friendly alternative to the conventional citric acid recovery process, that gives rise to enormous amounts of calcium sulphate (circa 2 kg of $CaSO_4.2H_2O$ per kg of monohydrated citric acid) that are to be disposed (Moresi and Sappino, 1998).
Table 1 summarises the main industrial ED applications in the food sector.

3. Mathematical Modelling

To design or optimise an ED process several parameters are to be taken into account, namely stack construction and spacer configuration, operation mode, membrane perm-selectivity, feed and product concentration, flow velocities, current density and voltage applied to the electrodes, recovery rates, etc. Most of the parameters of which are to be determined by independent experiments or existing correlations.
The Maxwell-Stefan (MS) equation represents the simplest mathematical tool for linking the flux of a generic species through the membrane with its interfacial concentrations at the membrane left- and right-sides, as well as with the external electrical voltage applied to the ED electrodes (Krishna and Wesselingh, 1997). To overcome the main problem in the application of the MS mass transfer model to ED processes, i.e. the large number of species diffusivities in the free solution and membrane phase (van der Stegen *et al*., 1999), the Nerst-Planck (NP) relationship is largely used to describe diffusion and electro-migration contributions to ion transport in ion-exchange membranes. The basic mathematical model consists of water and solute mass balances coupled with the solute and water transfer equations and voltage equation for the ED loop concerned, as given below:

$$\frac{d(n_{BC})}{d\theta} = -\frac{d(n_{BD})}{d\theta} = J_B\, a_{me}\, N\,;\quad \frac{d(n_{WC})}{d\theta} = -\frac{d(n_{WD})}{d\theta} = J_W\, a_{me}\, N \qquad (1)$$

$$J_B = \frac{t_s}{F} j - L_B\, \Delta c_B\;;\quad J_W = \frac{t_W}{F} j - L_W\, \Delta c_B \qquad (2)$$

$$E - E_{el} + (E_j + E_D) N_c = RI \qquad (3)$$

$$R = (R_c + R_{fc,D} + R_D + R_{fa,D} + R_a + R_{fa,C} + R_C + R_{fc,C}) N_c + 2R_{ERS} \qquad (4)$$

where all symbols are given in section 7.
The contribution of solute polarisation, namely the electric resistance (R_f) and junction potential difference (E_j) across any boundary layer, was found to be negligible, this being also true for the contribution of solute and water diffusion: $L_B \approx L_W \approx 0$ (Fidaleo and Moresi, 2004). On the contrary, the Donnan potential difference (E_D) in any cell pair, which behaves as a direct current generator with inverted polarities with respect to those of the external DC generator, has to be accounted for Δc_B increases:

$$E_D = 2\, t_s \frac{R_G\, T_K}{F} \ln\left(\frac{c_{BD}}{c_{BC}}\right) \qquad (5)$$

The ohmic resistances of the bulk solutions in the concentrating (C), diluting (D), or electrode rinsing solution (ERS) compartment can be estimated via the 2nd Ohm's law:

$$R_C \approx \frac{h}{a_{me}\, c_{B,C}\, \Lambda(c_{B,C})}\;;\; R_D \approx \frac{h}{a_{me}\, c_{B,D}\, \Lambda(c_{B,D})}\;;\; R_{ERS} = \frac{h_{ERS}}{a_{ERS}\, c_{B,ERS}\, \Lambda(c_{B,ERS})} \qquad (6)$$

The so called limiting current density (j_{lim}) is the first value at which the electrolyte concentration at an anionic (a) or cationic (c) membrane surface falls to zero. Its controlling values generally refer to the diluting compartments and can be estimated as:

$$j_{lim,c} = \frac{F\, c_{BD}\, k_m}{(t_c^+ - t^+)} \qquad j_{lim,a} = \frac{F\, c_{BD}\, k_m}{(t_a^- - t^-)} \qquad (7)$$

The solute mass transfer coefficient can be calculated by resorting to the empirical correlation previously developed (data not published):

$$Sh = (0.53 \pm 0.01)\, Re^{1/2} \cdot Sc^{1/3} \qquad (8)$$

4. Experimental Procedure

In this PhD thesis a five-step experimental procedure was set up by performing in sequence the following independent tests, that is i) zero-current leaching, osmosis, and dialysis; ii) electro-osmosis; iii) desalination; and iv) current-voltage tests. A fifth step was added to perform a few further trials (validation tests) to check for all the parameters estimated. In this way, it is possible to determine sequentially the main physical properties (ρ; η; π; χ; Λ; $\gamma^{\pm}$; D_B) of the free salt solutions by resorting to either the open literature or direct measurements; the membrane constants for solute (L_B) or water (L_W) transport by diffusion via tests i); the effective solute (t_s) and water (t_W) transport numbers in membranes by tests iii) and ii), respectively; the limiting current intensity (I_{lim}), ion transport numbers (t_a^-, t_c^+), and surface resistances (r_a, r_c) in anionic and cationic membranes, and solute mass transfer coefficient (k_m) by step iv).

5. Materials and Methods

A laboratory-scale electrodialyser (Aqualyzer P1, Corning EIVS, Le Vesinet, F), previously described (Moresi and Sappino, 1998), was used. Several batch recycle runs were carried out by varying electric current intensity (I=0.5-1.5 A) under constant feed solute concentration ($C_B \approx 0.5$ M), superficial velocity (v_S=3 cm s^{-1}), and temperature (T=293 K). The instantaneous salt concentrations in diluting (D) and concentrating (C) streams were indirectly estimated by measuring the electric conductivity (χ) at 293 K with a WTW conductivity meter mod. Inolab Cond Level 1. Limiting current tests at 293 K were performed to plot voltage (Φ)-current (I) curves using stacks composed of 19 cation- (CMV) or 19 anion-(AMV) exchange membranes by varying C_B, I and v_S.

5. Results and Discussion

5.1 Conductivity measurements

For strong binary electrolytes, the transport numbers for cation (t^+) and anion (t^-) in dilute solutions can be easily estimated from the equivalent conductance at infinite dilution ($\Lambda_o=\lambda_o^+ + \lambda_o^-$), as extrapolated from the plot of the experimental equivalent conductance ($\Lambda=\chi/C_B$) *vs*. the square root of solute molar concentration ($\sqrt{C_B}$) at 293 K, the Na^+ equivalent conductance at infinite dilution (λ_o^+) being equal to 44.95 S cm^2 mol^{-1} (Prentice, 1991). In this way, the transport numbers for Na^+ were calculated as shown in Table 2, while those for the anion were their corresponding complement to one.

Table 2 *ED recovery of some sodium salts from model solutions: effect of the salt molecular mass (M_S) on the main design parameters (i.e., t^+, t_s, t_W, a_{me}, r_a, r_c, t_c^+, t_a^-, ε).*

Salt	M_S (Da)	t^+	t_s	t_w	a_{me} cm^2	r_a Ω cm^2	r_c	t_c^+	t_a^-	ε Wh g^{-1}
NaCl	58.4	0.40	0.969±0.002	9.31 ± 0.07	49 ± 2	5.9	6.3	0.99	0.97	0.19
Na-A	82.0	0.56	0.931±0.003	14.8 ± 0.1	52 ± 1	12.0	6.0	0.93	1.00	0.21
Na-P	96.1	0.59	0.982± 0.002	15.23 ± 0.04	50 ± 1	19.1	6.3	0.95	1.03	0.20
Na-L	112.1	0.60	0.876± 0.002	15.60 ± 0.05	41 ± 3	16.4	5.5	0.92	0.96	0.22

5.2 Desalination tests

By plotting the net increment (or decrement) in C or D solute (Δn) or water (Δn_W) masses *vs.* the Faraday equivalents of solute transferred (n_F=NI θ/F), as shown in Fig. 1, it was possible to estimate t_s and t_W, for each salt studied (Table 2).

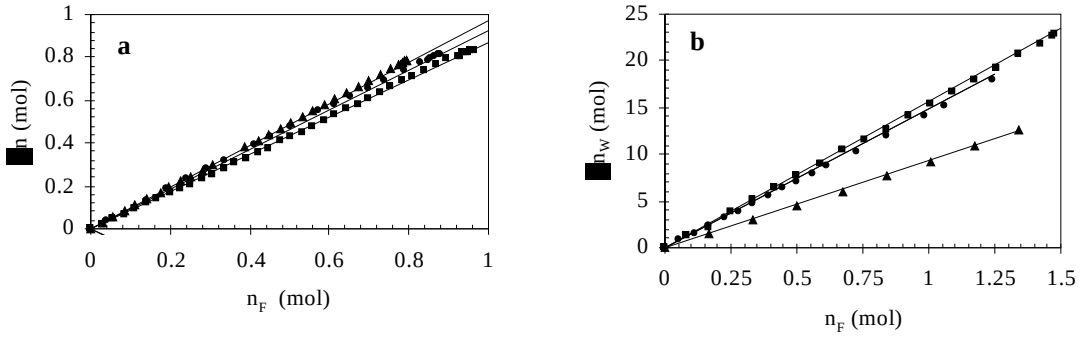

Figure 1 *Net increment in C solute (**a**) and water (**b**) masses for NaCl (▲), NaA (●) and, NaL (■) vs. the Faraday equivalents of solute transferred (n_F) using 10 AMV and 9 CMV membranes at 20°C, v_S=3 cm s^{-1} and I=1 A.*

5.3 Voltage-current tests

A series of E-I experiments using cationic or anionic membranes allowed the limiting current intensity ($I_{lim,c}$ or $I_{lim,a}$) and overall stack resistance to be determined. By plotting $I_{lim,c}$ or $I_{lim,a}$ vs. the solute concentration (C_B), two

linear graphs can be obtained (Fig. 2a). The ratios between their corresponding slopes $I_{lim,c}/I_{lim,a}=(t^+_a-t^+)/(t^-_c-t^-)$ were calculated as suggested by Krol *et al*. (1999) and used to estimate the anion transport numbers in the anionic membranes (Table 2). The current within the electro-membranes was almost exclusively carried by the counter ions.

For v_S ranging from 3.0 to 6.1 cm s^{-1}, E-I curves were coincident and linear with constant intercepts (i.e. $E_{el}\approx$2.2-2.6 V) and slopes for $I<0.75\ I_{lim}$, this being an indirect confirmation of negligible contribution of solute polarisation.

By neglecting the contribution of E_j, E_D and R_f, it was possible to establish two linear relationships between the apparent resistance (R_{MP}) of the anionic or cationic membrane pack and the reciprocal of the solution electrical conductivity (χ) (Fig. 2b) with intercept and slope respectively proportional to the resistance (r_m) of the electro-membrane concerned and membrane gap per unit effective membrane surface area (h/a_{me}). Fitting each set of data via the least squares method yielded the specific membrane resistances shown in Table 2. The estimated values of a_{me} were practically coincident with the exposed surface area of electrodes (44.6 cm^2) and significantly different from the geometrical membrane surface area (72 cm^2).

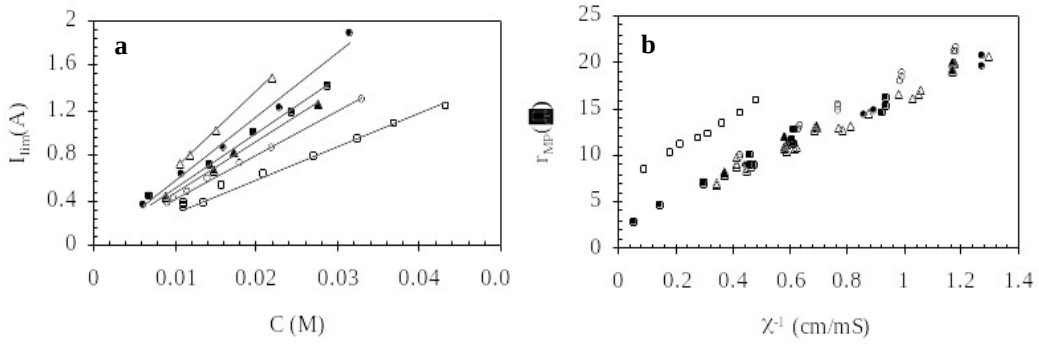

Figure 2 *Main results of limiting current tests for NaCl* (▲, Δ), *NaA* (● , ❍), *NaL* (■, ☐) *as referred to cationic (closed symbols) or anionic (open symbols) membranes:* **a**) *limiting current intensity (I_{lim}) vs. solute molar concentration (C);* **b**) *electrical resistance of membrane pack (r_{MP}) vs. the reciprocal of conductivity (χ).*

5.4 Validation tests

By integrating Eq.s (1) and (2) together with the above independent parameters and Eq.s (3)-(4), it was possible to calculate the instantaneous values of $c_B(\theta)$ in C and D tanks, as well as the voltage applied to the membrane pack ($\Phi_{MP}=E-E_{el}-2\ R_{ERS}\ I$). As an example, Fig. 4 shows quite a satisfactory agreement between the experimental (closed and open symbols) and calculated (continuous lines) values of $c_{BC}(\theta)$, $c_{BD}(\theta)$, and $\Phi_{MP}(\theta)$ against time (θ) in the case of sodium acetate removal.

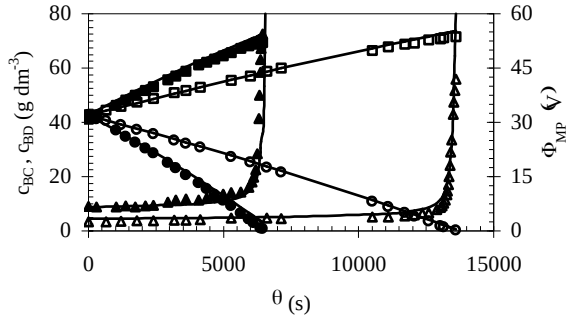

Figure 4 *Batch recovery of NaA using 10 AMV and 9 CMV membranes at 293 K, v_s=3 cm/s and I=0.75 A (open symbols) or 1.5 A (closed symbols): solute concentrations in* C (c_{BC}: ■, ☐) and D (c_{BD}: ● , ❍) *streams, and voltage applied to the ED stack* (Φ_{MP}: ▲,△) *vs. time (θ).*

5.5 ED Recovery of some fermentation products

As the molecular mass (M_S) of solute increased from 58 to 112 Da, the transport number for Na^+ in the corresponding solution tended to increase from 0.4 to 0.6 for the progressively smaller equivalent conductance at infinite dilution of acetate, and lactate ions with respect to that of Cl^{-1}. Nevertheless, the current within the electro-membranes was almost exclusively carried by the counter ions. The effective solute (t_s) transport number, that is the Faraday efficiency, ranged from 93 to 98%, even if reduced to 88% for sodium lactate. Despite the water transport number (t_W) increased from 9.3 to 15.6, the maximum salt weight concentration in the concentrate ranged from 287 to 349 kg m^{-3}. Whereas the surface resistance (r_c) of the cationic membranes was about constant (6.0± 0.4 Ω cm^2), r_a tended to increase almost linearly with M_S (r^2=0.8), even if this yielded up to just a 15% increase in the specific electric energy consumption per kg of salt recovered (ε) in the case of 90% salt recovery at 1 A and 293 K (Table 2).

Finally, the membrane surface area (a_{me}) effectively utilised was found to be about two thirds of the geometrical one and just 10% greater than the exposed surface area of electrodes. This confirmed the general rule that recommends to provide the electrodes with bases with the highest degree of open area in the direction

perpendicular to the membrane faces so as to maximise utilisation of membrane area and minimise the electrical resistance of stack.

6. Conclusions and Future Perspectives

The present ED industry has experienced a steady growth rate of about 15% since 15 years. There are, however, a number of problems, that undoubtedly limit growth in membrane sales, like membrane fouling problems, design considerations, cleanability, investment and membrane replacement costs and competing technologies, such as nanofiltration (NF) and ion-exchange resins (IER). To overcome such uncertainties, long-term laboratory- and pilot-scale experiments are needed to assess membrane process performance and reliability.
For instance, in the food biotechnology sector ED applications are still in their infancy, since practically none of the processes studied in laboratory- and pilot-scales have been converted into industrial realities, except for the recovery of Na-L from clarified fermentation broths. This means that ED processing potentialities have not been completely exploited so far probably because of the high specific electro-membrane costs or their short lifetime.
The sequence of independent experimental trials outlined here is therefore recommended to estimate the really effective parameters for designing or optimising ED stacks. More specifically, the assessment of the effective membrane resistance, as well as surface area, appears to be of paramount importance if the data collected in a laboratory- or pilot-scale plant are to be safely transferred into an industrial-scale one. In this way, such an optimal strategy is expected to foster novel ED applications in the food sector, as well as in the chemical, pharmaceutical, and municipal effluent treatment areas.

7. Nomenclature

a_{me}, effective membrane surface area per each cell pair (m^2); c_B, C_B, solute weight and molar concentrations in C, D, or ERS compartment (mol m^{-3}); D_B, diffusivity (m^2 s^{-1}); E, overall potential drop across an ED stack (V); E_D and E_j, Donnan and junction potential differences across membranes (V); E_{el}, thermodynamic electrode potential (V); F, Faraday's constant (96,486 C mol^{-1}); h, membrane gap (m); h_{ERS}, electrode channel width (m); I, electric current intensity (A); I_{lim}, limiting current intensity (A); J_B and J_W, solute and water permeation fluxes (mol m^{-2} s^{-1}); j, electric current density (A m_{-2}); j_{lim}, limiting electric current density (A m_{-2}); k_m, solute mass transfer coefficient (m s^{-1}); L_B and L_W, membrane constant for solute or water transport by diffusion (m s^{-1}); M_S, molecular mass (Da); N_c, overall number of cell pairs; n_B and n_W, solute and water masses (mol); R, electric resistance (Ω); R_{ERS}, electric resistance of electrode rinsing solution (Ω); R_f, boundary layer electric resistance (Ω);R_G , gas-law constant (=8.31 J mol^{-1} K^{-1}); R_{MP}, apparent resistance of the generic membrane pack (Ω); Re, Reynolds number (= ρ v_S h/η); r_m, membrane surface resistance (Ω cm^2); Sc, Schmidt number [=η/(ρ D_B)]; Sh, Sherwood number (=k_m h/D_B); T_K, absolute temperature (K); t^- and t^+, transport numbers for anion and cation in solution; t_{m^-} and t_{m^+}, anion and cation transport numbers in a generic membrane; t_s, effective transport number; t_w , water transport number; χ, electric conductivity (S m^{-1}); $\gamma^{\pm}$, molal activity coefficient (dimensionless); Φ_{MP}, voltage applied to the membrane pack (V); Λ, equivalent conductance of the corresponding bulk solutions (=χ/c_B, m^2 mol^{-1}); η, viscosity (Pa s); θ, time (s); ρ, density (kg m^{-3}); π, osmotic pressure (Pa).

8. References

Fidaleo M, Moresi M (2004) Modelling the electrodialytic recovery of sodium lactate. *Biotechnol Appl Biochem* **40**: 1-9.

Ho WSW, Sirkar KS (1992) *Membrane technology*, New York: Chapman & Hall.

Krishna R, Wesselingh J A (1997) The Maxwell-Stefan approach to mass transfer. *Chem Eng Sci* **52**: 861-911.

Krol JJ, Wessling M, Strathmann H (1999) Concentration polarization with monopolar ion exchange membranes: current-voltage curves and water dissociation. *J Membr Sci* **162**: 145-154.

Moresi M, Sappino F (1998) Effect of some operating variables on citrate recovery from model solutions by electrodialysis. *Biotech Bioeng* **59**: 344-350.

Prentice G (1991) *Electrochemical Engineering Principles*, New Jersey (USA): Prentice-Hall International.

Shaposhnik VA, Kesore K (1997) An early history of electrodialysis with permselective membranes. *J Membr Sci* **136**: 35-39.

Spitz M (2004) Experimental strategy for the optimal design of electrodialysis units used to recover some fermentation products. In Proc.s of the 9th Workshop on the *Developments in the Italian PhD Research on Food Science and Technology*, Parma (Italy), 7-9 September, 2004, pp. X-Y.

van der Stegen JHG, van der Veen AJ, Weerdenburg H, Hogendoorn JA, Versteeg GF (1999) Application of the Maxwell-Stefan theory to the transport in ion-selective membranes used in the choralkali electrolysis process. *Chem Eng Sci* **54**: 2501-2511.

POSTER COMMUNICATIONS

Recovery of Selected Microbial Metabolites from Model Solutions by Reverse Osmosis

John Smith (jsmith@unibus.it)
Dept. Food Science and Technology, University of XXX, VYUUU, Italy
Tutor: Prof. X Y

The first two activities of the PhD thesis project are described. Firstly, the density, viscosity, and osmotic pressure of aqueous solutions of sodium citrate, gluconate, and lactate were determined and correlated to the solute molar concentration (C_B). Secondly, recovery of such solutes from aqueous solutions was studied batchwise in a pilot plant equipped with a spiral-wound thin-composite reverse osmosis membrane, thus assessing that the osmotic pressure is the major resistance to overcome.

Recupero di alcuni metabolici microbici da soluzioni modello per osmosi inversa

Le prime 2 attività del progetto di tesi di dottorato sono descritte. Sono state determinate la densità, la viscosità e la pressione osmotica (π) di soluzioni acquose di citrato, gluconato e lattato di sodio, correlandole alla concentrazione molare di soluto (C_B). Si è studiato il recupero in batch di questi soluti in un impianto pilota, impiegando un modulo di osmosi inversa a spirale e si è ricavato che la permeazione del solvente è limitata da π.

Key words: Reverse osmosis, sodium citrate, gluconate, and lactate, membrane resistance, process modelling.

1. Introduction

In accordance with the PhD thesis project previously decribed (Fddff, 2005), this poster reports the main results of the first two activities concerning:

(A1) the determination and modelling of the density (ρ), kinematic viscosity (ν), and osmotic pressure (π) of di-sodium hydrogen citrate, sodium gluconate, and sodium lactate in aqueous solutions as functions of feed weight (c_B) or molar (C_B) solute concentration;

(A2) the assessment and modelling of the RO processes in a pilot-plant scale equipped with a spiral-wound membrane module as functions of transmembrane pressure difference applied (ΔP), and C_B.

2. Materials and Methods

A typical temperature- and pressure-controlled pilot-scale RO plant (VERIND, Rodano, I), previously described (Lo Presti and Moresi, 2000), was used. It was equipped with a thin-film composite spiral-wound membrane module, type SW30-2514 (FilmTec Corp., Div. of Dow Chemicals, Minneapolis, MN, USA) with 0.762-mm and 250-mm channel width and length, and 0.42-m^2 effective surface area. Several batch recycle runs were carried out under constant recirculation flow rate (1 $m^3\ h^{-1}$) and temperature (T=313 K) by varying ΔP from 40 to 60 Pa. The feed solutions were prepared by dissolving technical grade di-sodium hydrogen citrate, sodium gluconate in or diluting 90% w/w lactic acid solution with deionised water to vary c_B in the range 50-75 kg m^{-3} to simulate the corresponding clarified fermentation medium. The pH of all acidic solutions was set to 5 by adding NaOH. The osmotic pressure (π) at 310K, kinematic viscosity (ν) at 313K, and density (ρ) at 293K of several aqueous solutions containing 0-1.6 kmol m^{-3} of the above salts were determined by using a Wescor Vapor Pressure osmometer (mod. 5500), capillary #25-50 Cannon-Fenske viscometers (ASTM, 1964), and calibrated volumetric flasks, respectively. The membrane module was cleaned and stored according to Lo Presti and Moresi (2000).

3. Results and Discussion

3.1 Determination of the main physical properties

The physical properties of the solutions tested were correlated to c_B or C_B as follows:

$$\rho = \rho_w + c_B(1 - \rho_w/\rho_B) \quad (1)$$

$$\mu_r = \mu/\mu_W = \exp(aC_B + bC_B^2) \qquad \pi = \alpha C_B \quad (2)$$

where ρ_W and ρ_B are the densities of pure water and pure solute; μ and μ_W are the solution and water dynamic viscosities; μ_r is the relative viscosity; C_B the solute molar concentration; a and b are empirical coefficients; π is the solution osmotic pressure, and α is known as the first "virial coefficient". All unknown parameters were determined using the least squares method, as reported in Table 1.

Table 1 *Empirical correlations of the density, relative viscosity, and osmotic pressure of several aqueous solutions of the Na salts of citric, gluconic, and lactic acids for C_B ranging from 0 to 1.8 kmol m^{-3}.*

Solute	Density ρ_B (kg m^{-3})	r^2	Relative a (m^3 kmol^{-1})	viscosity b (m^6 kmol^{-2})	r^2	Osmotic Pressure α (Pa m^3 kmol^{-1})	r^2
Citrate	2106	0.999	0.64±0.09	0.16±0.01	0.999	56.7±1.2	0.990
Gluconate	1919	0.997	0.56±0.02	0.16±0.02	0.998	47.9±0.5	0.996
Lactate	1321	0.977	0.68±0.07	0.23±0.09	0.972	60.7±1.1	0.993
All solutes tested	-		0.52±0.04	0.15±0.03	0.983	4.3±1.0	0.967

3.2 Modelling of the RO process

According to conventional filtration theory (Cheryan, 1998), the actual mass flux of permeation (J_p) through the membrane is given by:

$$J_p = (\Delta P - \Delta\pi) / [\nu (R_m + R_f + R_g)] \quad (3)$$

with

$$\Delta P = P_m - P_p = 1/2 (P_i + P_o) - P_p \quad (4)$$

where ΔP is defined as the difference between the average pressures in the retentate (P_m) and permeate (P_p) sides, the former being the half sum of the inlet (P_i) and outlet (P_o) pressures in the retentate side; R_m is the intrinsic membrane resistance, and R_f or R_g is the membrane resistance due to fouling or polarisation layer. In particular, Eq. (4) was modified by replacing the solvent kinematic viscosity with the retentate one to account for its increase with C_B (Lo Presti and Moresi, 2000). Moreover, in accordance with Eq. (3) and Table 1, the instantaneous osmotic pressure difference between the retentate and permeate ($\Delta\pi$) was estimated as proportional to the difference between the retentate and permeate solute concentrations at the membrane surfaces.

The intrinsic membrane resistance (R_m) was determined by performing several deionised water permeation tests at different ΔP (10-60 Pa) and T (303-313K) values, thus obtaining the following empirical regression:

$$R_m = (-8.90 \pm 0.13) \cdot 10^{12} T + (7.31 \pm 0.04) \cdot 10^{14} \qquad r^2 = 0.99 \quad (5)$$

Whatever the solute under study, the evolution of the RO concentration process was characterised by a similar decline in J_p as C_B increased (Fig. 1). This was the direct result of the strict similarity of the π-C_B relationships for all the solutes examined (Table 2).

In all cases, the apparent solute rejection (Cheryan, 1998) was found to be greater than 99%, thus allowing the solute concentration in the permeate to be regarded as virtually zero (C_{Bp}=0). Moreover, feed flow rate exhibited little or no effect on J_p, thus enabling the contribution of polarisation layer to be neglected (R_g=0). On the contrary, the contribution of fouling deposited onto the membrane (R_f) tended to increase with time. As it got to about one third of the intrinsic membrane resistance, a conventional chemically-based cleaning procedure was capable of restoring the intrinsic membrane resistance of the new membrane.

Fig. 1 shows the experimental permeation fluxes *vs*. C_B measured during subsequent batch RO concentration trials of all salts tested as compared to those calculated using the model reported here. Such a modelling exercise might be helpful to optimise the recovery of microbial metabolites from clarified fermentation broths. Thus, the experimental results agree with the expected ones and the original PhD thesis project can proceed without any substantial amendment.

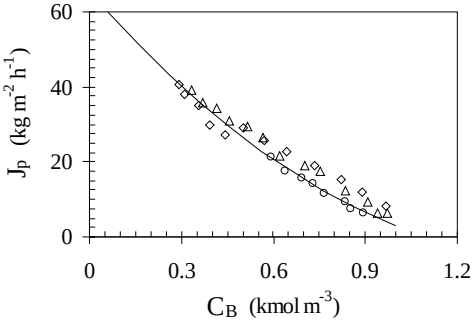

Figure 1 *Effect of C_B on J_p during the RO concentration of sodium-citrate (Δ), -gluconate (◊), and -lactate (○) under the following operating conditions: feed flow rate (1000 dm^3/h), T=313K, and P_i=6.1 MPa. The continuous line was calculated as reported in the text.*

4. References

ASTM (1964) Standard method of test for kinetic viscosity (ASTM D445-IP 71). In ASTM Standards -Electrical Insulating Materials - Part 29, Baltimore (USA): American Society for Testing and Materials, pp. 312-363.

Cheryan M (1998) *Ultrafiltration and Microfiltration Handbook*, Lancaster (USA): Technomic Publ. Co.

Lo Presti S, Moresi M (2000) Recovery of selected microbial metabolites from model solutions by reverse osmosis. *J Membr Sci* **174**: 243-253.

Smith J (2005) Experimental strategy for the optimal design of ultrafiltration units used to recover some food biopolymers. In Proc.s of the 10th Workshop on the *Developments in the Italian PhD Research on Food Science and Technology*, Foggia (Italy), 7-9 September, 2005, pp. X-Y.

PhD DISSERTATION PROJECTS

Experimental Strategy for the Optimal Design of Ultrafiltration Units Used to Recover Some Food Biopolymers

Arnold Schwartz (aschwartz@unibus.it)
Dept. Food Science and Technology, University of XXX, VYUUU, Italy
Tutor: Prof. X Y

This PhD thesis research project is aimed at setting up a batch or total recycle experimental procedure at both bench-top and pilot scales to identify the most appropriate mathematical model to simulate accurately the recovery of selected food biopolymers via tubular or hollow-fibre ultrafiltration modules and provide a basis for their optimal design in an industrial scale.

Strategia sperimentale per la progettazione ottimale di unità di ultrafiltrazione per il recupero di biopolimeri di interesse alimentare

Questo progetto di tesi di dottorato mira a mettere a punto un procedimento sperimentale, in batch o a riciclo totale, prima in impianto da banco e poi in impianto pilota, atto ad individuare il modello matematico in grado di simulare il processo di recupero di selezionati biopolimeri di interesse alimentare mediante moduli a membrana di ultrafiltrazione tubolari o a fibre cave, consentendone il dimensionamento ottimale in scala industriale.

1. State-of-the-Art

Since the early 60s membrane separation processes have presented quite a limited diffusion and have just more recently begun to be recognised as efficient, economical and reliable separation processes. Depending on membrane pore size, feed cross flow velocity, transmembrane pressure difference applied (ΔP) and permeation flux, membrane filtration processes can be classified as microfiltration (MF), ultrafiltration (UF), nanofiltration (NF), and reverse osmosis (RO), the configuration of their modules being *tubular* (T), *hollow-fibre* (HF), *spiral-wound* (SW) or *plate-and-frame* (PF) (Cheryan, 1998; Daufin *et al*., 1998; Ho and Sirkar, 1992).
Table 1 lists the main applications of UF membrane processing in the food and beverage sector together with specific membrane type and configuration, range of solvent permeation flux (J_{Wv}) and solute true rejection (r_t) .
A great number of problems limit UF membrane sale growth like membrane resistance to solvent, fouling problems, design considerations for the incomplete comprehension of mass transfer mechanisms in membrane systems, cleanability, investment and membrane replacement costs, and competing technologies. Formation of a gel-polarised layer onto membrane surface, as well blocking of membrane surface pores or fouling of support materials, results in a more or less pronounced permeation flux decay. Such a decay is still difficult to quantify at the design stage by resorting to any of the numerous transport models available in the literature, that is *non porous or homogeneous membrane models* (*i.e.* solution-diffusion, extended solution-diffusion, and solution-diffusion-imperfection models), *pore-based models* (preferential sorption-capillary flow, finely porous, and surface force-pore flow models), and *irreversible thermodynamics phenomenological models* (such as Kedem-Katchalsky and Spiegler-Kedem models).

Table 1 Main applications of UF membrane processes in the food sector.

Application	**Example**	**Membrane module characteristics**				
		Type	**Material**	**Cut-off** (kDa)	**J_{wv}** ($dm^3\ m^{-2}\ h^{-1}$)	**r_t** (%)
Fractionation	Milk or whey (protein from lactose and minerals)	PF, SW, T	C, PS, PES	10-100	5-100	70-97
	Oil fractions from oil-in-water emulsions	SW	TFC	8	10-13	70-90
Clarification	Alcoholic juices and beverages	HF, SW, T	PAN, PS, PES	10-100	5-100	70-97
	Removal of colloids, pigments, low MW compounds	HF, T	PAN, PES	10-50	5-50	70-83
Concentration	Albumin and proteins	PF, SW, T	C, PS, PES	10-100	5-30	70-83
	Polysaccharides (karragineen, xanthan)	HF	PS	500	5-10	-

C: Ceramic; PS: Polysulfone; PES: Polyethersulfone; PAN: Polyacrylonitrile; TFC: Thin Film Composite.

For instance, it is difficult to express the real relationship between J_{Wv} and ΔP and, in particular, the fact that in the UF range J_{Wv} is controlled by pressure for $\Delta P<6$ Pa and by mass transfer for $\Delta P>6$-10 Pa, this effect being counteracted by increasing feed flow rate (Q_F) or process temperature (T), as well as decreasing feed solute

concentration (C_B). Moreover, while in the RO range J_{wv}-logC_B plot linearly decreases with C_B increasing and vanishes for C_B as such that the feed osmotic pressure equals feed input pressure, in the UF range such a plot does not tend to zero, but it may reach a minimum value (definitively different from zero), which remains practically constant or increases up to a maximum value before finally decreasing as solute concentration increases (Pritchard *et al.*, 1995).

Almost all the biopolymers recovered via UF processes exhibit a non-Newtonian behaviour of the pseudoplastic type. This is generally described via the Ostwäld-de Waele model, that allows a quite accurate reconstruction of the liquid apparent viscosity (η_a) in the intermediate shear rate region only, but at very low shear rates overestimates η_a, thus leading to mass transfer coefficients extremely underestimated. Thus, this PhD thesis project will be directed to select which mathematical model with the minimum number of statistically independent parameters allows the best reconstruction of UF membrane process performances buy resorting to well known experimental design techniques to minimise the experimental trials needed.

2. PhD Thesis Objectives and Milestones

Within the overall objective mentioned above this PhD thesis project can be subdivided into the following activities according to the Gantt diagram given in Table 2:

A1) **Determination of the physical properties of a few selected biopolymers** (sodium alginates and pectinate, and whey proteins) in aqueous solutions to model their density, osmotic pressure (A1.1) and rheological behaviour (A1.3) as functions of C_B.

A2) **Assessment and modelling of the UF processes in a bench-top plant scale** to identify the mathematical model capable of reconstructing their performances as functions of the main operating variables (ΔP; T; Q_F, C_B) and membrane constitution, porosity and configuration, that is a C-T (A2.1) and a PES HF (A2.2) membrane module. An experimental strategy to limit polarisation layer growth will also be established to optimise both UF module performance.

A3) **Scaling-up of the UF processes** in the pilot plant scale to validate the prediction capability of mathematical models identified during activity A2 when using commercial C-T (A3.1) and PES-HF (A3.2) UF membrane modules.

A4) **Optimisation of the UF processes examined** so as to assess their optimal operating conditions (A4.1) and set up a generalised experimental procedure (A4.2) to determine the main engineering parameters necessary to design the UF unit in an industrial scale.

A5) **Writing and Editing** of the PhD thesis, scientific papers and oral and/or poster communications.

Table 2Gantt diagram for this PhD thesis project.

Activity — Months		**1**	**2**	**3**	**4**	**5**	**6**	**7**	**8**	**9**	**10**	**11**	**12**	**13**	**14**	**15**	**16**	**17**	**18**	**19**	**20**	**21**	**22**	**23**	**24**
A1)	***Biopolymer Physical Properties***																								
	1) Density, Osmotic Pressure																								
	2) Rheological Behaviour																								
A2)	***UF Process Modelling***																								
	1) Ceramic Tubolar Module																								
	2) Hollow-fibre Module																								
A3)	***Scaling-up of UF processes***																								
	1) Ceramic Tubolar Module																								
	2) Hollow-fibre Module																								
A4)	***UF Process Optimisation***																								
	1) Optimal UF Processes																								
	2) Generalised Exp.l Procedure																								
A5)	***Thesis and Paper Preparation***																								

3. Selected References

Cheryan M (1998) *Ultrafiltration and Microfiltration Handbook*, Lancaster (USA): Technomic Publ. Co.

Daufin G, René F, Aimar P (1998) *Les séparations par membrane dans les procédés de l'industrie alimentaire*, Paris: Technique & Documentation Lavoisier.

Ho WSW, Sirkar KS (1992) *Membrane technology*, New York: Chapman & Hall.

Pritchard M, Howell JA, Field RW (1995) The ultrafiltration of viscous fluids. *J Membr Sci* **102**: 223-235.